ChemComm

COMMUNICATION

View Article Online
View Journal

Cite this: DOI: 10.1039/d3cc05487j

Received 7th November 2023,
Accepted 27th November 2023

DOI: 10.1039/d3cc05487j

rsc.li/chemcomm

A DNA rotary nanodevice operated by enzyme-initiated strand resetting†

Arun Richard Chandrasekaran

DNA nanostructures that respond to external stimuli have found applications in several areas such as biosensing, drug delivery and molecular computation. The use of different types of stimuli in a single operation provides another layer of control for the reconfiguration of nucleic acid nanostructures. This work demonstrates the use of a ribonuclease to "unset" a nucleic acid nanodevice based on the paranemic crossover (PX) DNA and specific DNA inputs to "reset" the structure into a juxtaposed DNA (JX_2) configuration, resulting in a 180° rotation of the helical domains. Such operations would be useful in translational applications where DNA nanostructures can be designed to reconfigure on the basis of more than one stimulus.

Creation of stimuli-responsive DNA nanostructures holds applications in diagnostics, drug delivery and molecular computation.[1] Typically, this is achieved by changing solution conditions (*e.g.*: pH[2] or temperature[3]), physical stimuli (*e.g.*: light[4] or force[5]) or by the interaction of other biomolecules (*e.g.*: nucleic acids[6] and proteins[7]). In some cases, a combination of external stimuli is more advantageous, such as in producing circuits with minimal use of DNA strands or as a gated response in biosensing strategies.[8,9] Here, I present reconfiguration of a DNA nanodevice using a combination of ribonuclease and nucleic acids.

As a model system to demonstrate the strategy, I use a previously reported device based on paranemic crossover (PX) DNA and juxtaposed (JX) DNA.[10] The PX-JX_2 device is sequence-dependent, where each state is controlled by the hybridization topology of specific "set" strands (Fig. 1). The PX state contains two adjacent double helical domains connected by five strand crossovers. The JX_2 state lacks two crossovers compared to the PX state. Further, the PX and JX_2 states differ from each other by a half turn rotation, causing a 180° rotation of one end of the structure relative to the other (denoted by C and D in Fig. 1). In prior work, interconversion between the PX and JX_2 states was achieved by toehold-based DNA strand displacement, with the set strands containing a DNA toehold that is free to bind a pair of displacing strands[10] as well as a version where the toeholds are protected by an RNA complement.[11] The rotational difference between the helical domains in the PX and JX_2 states has been previously shown by atomic force microscopy of a one-dimensional array and the device has been used in prototyping DNA synthesis,[12] arrangement of metallic nanoparticles[13] and in a molecular assembly line.[14] In this work, I incorporate RNA strands directly into the PX structure and use a combination of ribonuclease H (RNase H) and DNA strands to operate the PX-JX_2 device, as an alternative to toehold-based strand displacement process.

The schematic and molecular models of the structures used in this study are shown in Fig. 1. The PX state of the device contains two long strands set in the PX configuration by two RNA set strands (Fig. 1 and Fig. S1, ESI†). In a paranemic structure, the alternating arrangement of major and minor grooves are wide and narrow respectively for PX DNA,[15] while in a PX RNA, the double helix has a narrow but deep major groove and a wide but shallow minor groove.[16] The motif used here has partial characteristics, where some regions are all-DNA and the set strand bound regions in the PX state have the properties of DNA–RNA hybrids. Addition of RNase H degrades the RNA set strands that are part of the DNA/RNA hybrid region, changing the device from the PX state to the naked frame intermediate. A pair of DNA set strands can now be added to reset the naked frame into the JX_2 state. Once the device is converted from the PX to the JX_2 state, the lower double helical domains of the device are turned 180° related to the starting configuration.

The sequences of the PX and JX_2 structures used here are adapted from a previous study[11] and modified to suit this work (Table S1, ESI†). I first assembled the PX and JX_2 states separately by annealing the component DNA strands and validated proper assembly of the structures using non-denaturing polyacrylamide gel electrophoresis (PAGE) (Fig. 2a). Further, the PX structure containing the RNA set strands showed a single band indicating

The RNA Institute, University at Albany, State University of New York, Albany, NY, 12222, USA. E-mail: arun@albany.edu

† Electronic supplementary information (ESI) available: Materials, methods, and additional experimental results. See DOI: https://doi.org/10.1039/d3cc05487j

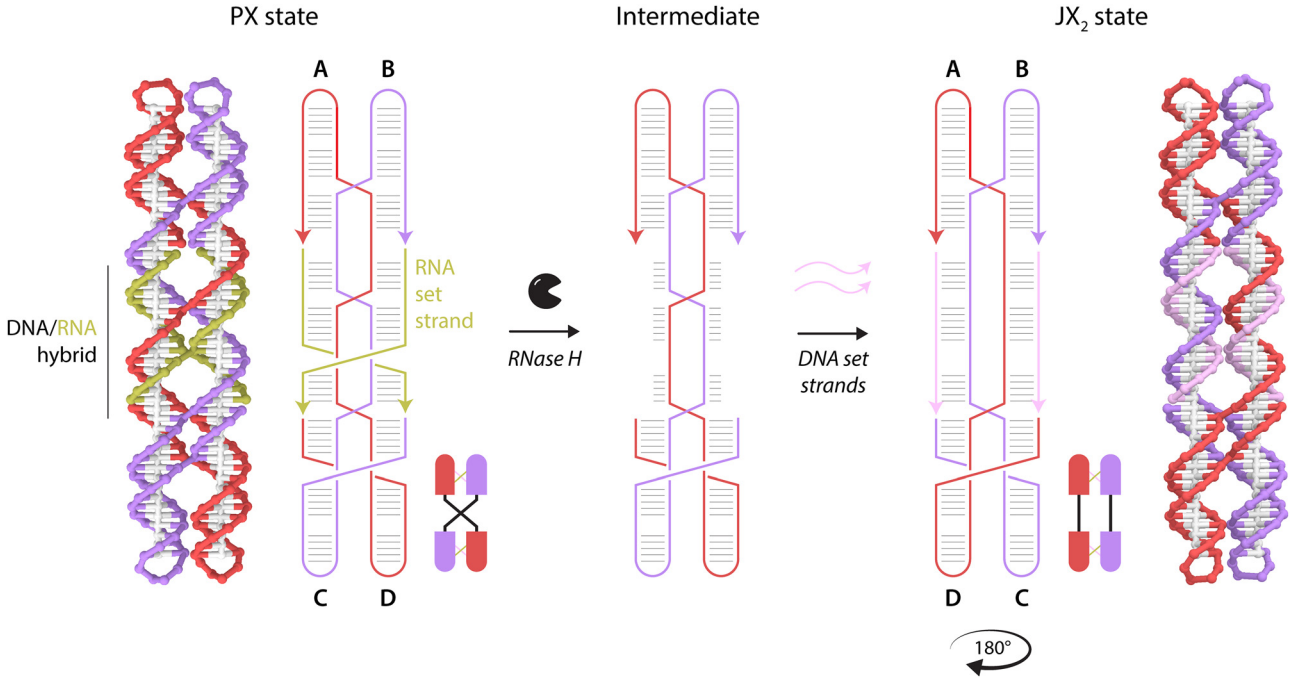

Fig. 1 Operation of the PX-JX_2 device. Schematic shows the ribonuclease-induced unsetting of PX state of the device to a naked frame intermediate, followed by addition of DNA strands that reset the device in the JX_2 state. Molecular models of the PX and JX_2 states are also shown. The two set strands are composed of different sequences but are shown in the same color for PX or JX_2 state for simplicity.

proper assembly compared to an all-DNA PX structure (Fig. S2, ESI†). I then analyzed the different states by comparing their mobilities as a function of polyacrylamide concentration using a Ferguson plot (Fig. 2b), where the slope provides an estimate of the frictional coefficient of the structures. I compared the PX state, JX_2 state and the 100 bp band of a 10 bp marker (which is a duplex roughly similar in size to the PX and JX_2 states). The PX structure is more compact compared to the JX_2 structure and migrates faster through the gel, a characteristic observed in my previous work comparing PX, JX_2 and DX motifs[17] as well as other works related to the PX-JX_2 device.[10,18,19] This difference in migration allows convenient observation of the reconfiguration between the two structures.

Next, I tested whether RNase H could be used to digest the RNA set strands and thus "unset" the PX state to the naked frame intermediate (Fig. 3a). I incubated the assembled PX state of the device with RNase H at 20 °C for 1 hour, followed by the addition of JX_2 set strands and incubation at 20 °C for 1 hour. While the optimal temperature for RNase H is 37 °C, my previous work showed that RNase H works sufficiently well at room temperature,[20] allowing its use with DNA nanostructures for isothermal reactions at 20 °C (note that both PX and JX_2 structures of a different size range have been shown to be stable at 37 °C).[17] Results showed complete conversion of the PX state into the JX_2 state (Fig. 3b). As a control, I tested the PX structure assembled with DNA set strands and treated it with RNase H. Addition of JX_2 set strands after RNase H treatment did not have any effect and the structure remained in the PX state, showing that the incorporation of RNA set strands makes this operation input specific (Fig. 3b).

I then optimized the concentrations of RNase H and set strands required for reconfiguration. I incubated the PX state of the device with different amounts of RNase H for 30 min, followed by addition of JX_2 set strands (Fig. 3c and Fig. S3, ESI†). With 5 units of RNase H, I observed complete PX to JX_2 conversion and used this enzyme amount for further experiments (Fig. 3c, inset). Next, I incubated RNase H-treated PX samples with different ratios of the JX_2 set strands. Even with 1 : 1 ratio of the PX to set strands, I observed full conversion of the intermediate to the JX_2 state (Fig. 3d and Fig. S4, ESI†). This is in contrast to strand displacement based reconfiguration where higher ratios of the displacing strands are needed.[10] Further, resetting of the RNase H-treated PX to JX_2 state occurs within a few minutes even with 1 : 1 ratio of PX : JX_2 set strands (Fig. 3e and Fig. S5, ESI†). For potential use in biological applications, I then tested whether the device can be operated

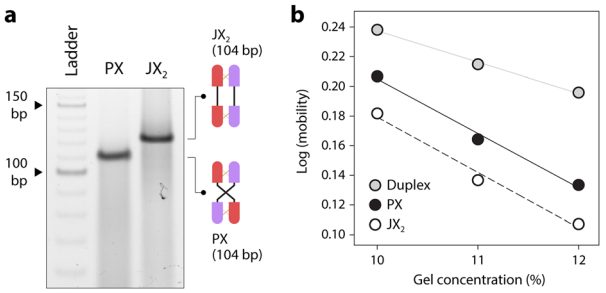

Fig. 2 Assembly and characterization. (a) Non-denaturing gel showing the assembly of the PX and JX_2 states. (b) Ferguson plot analysis comparing the PX and JX_2 states and a double-helical molecule of similar length.

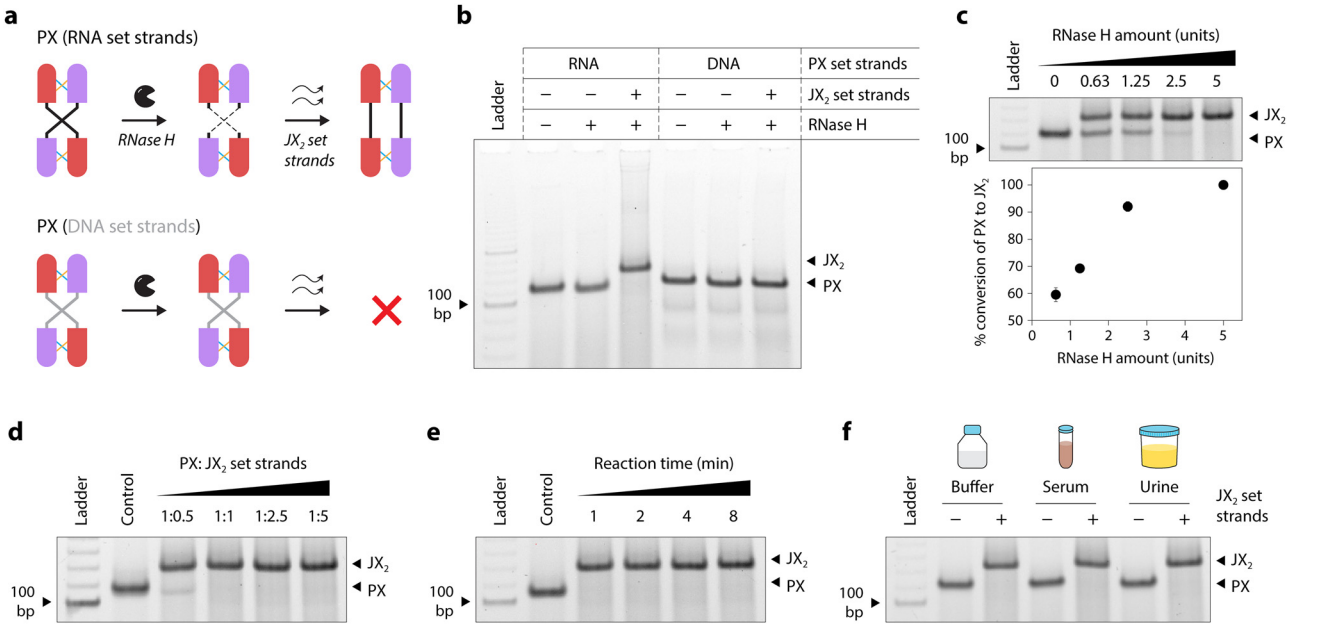

Fig. 3 RNase-initiated operation of the device. (a) Schematic showing resetting of the PX state to the JX_2 state by RNase H and set strands. (b) Non-denaturing gel showing reconfiguration of the PX-JX_2 device. (c) RNase H concentration series for resetting the PX device. (d) Different ratios of JX_2 set strands used to reconfigure the intermediate frame to the JX_2 state. (e) Time series for reconfiguration of the intermediate frame to the JX_2 state on addition of JX_2 set strands. (f) Operation of the device in biofluids. Full images for gels are shown in the ESI.†

in biological fluids. I incubated the PX state in either human serum or human urine, followed by RNase H treatment and the addition of JX_2 set strands (Fig. 3f and Fig. S6, ESI†). Reconfiguration was successful in both cases, with complete conversion as observed in buffer.

This work provides an example for using combinatorial inputs to operate nucleic acid devices. Such operations would be useful in translational applications where DNA nanostructures can be designed to reconfigure on the basis of more than one stimulus (enzyme and nucleic acids in this case). With further modifications, this system can be made reversible by using RNA set strands for both the PX and the JX_2 states, where addition of RNase H changes the structures to the unstructured intermediate, which can then be "set" in either the PX or the JX_2 state with the addition of corresponding nucleic acid fuels. Such dissipative systems have recently been demonstrated for nucleic acid circuits and for the assembly and disassembly of DNA nanotubes using RNA producing or degrading enzymes.[21–23] Moreover, the use of RNA in the reconfiguration process can be combined with toehold-controlled reactions, such as the use of RNA blocker strands[22] or RNase-activated toehold clipping.[24] Overall, the functionality provided by RNA component strands and the rotational movement in the device could be combined with larger DNA nanostructures for time-delayed or stimuli-responsive mechanical operations that are useful in biosensing, drug delivery and molecular computation.

Research reported in this publication was supported by the National Institutes of Health (NIH) through National Institute of General Medical Sciences (NIGMS) under award number R35GM150672 to A. R. C. I thank Arlin Rodriguez for technical assistance.

Conflicts of interest

There are no conflicts to declare.

References

1 M. DeLuca, Z. Shi, C. E. Castro and G. Arya, *Nanoscale Horiz.*, 2020, **5**, 182–201.
2 W. Ji, D. Li, W. Lai, X. Yao, Md. F. Alam, W. Zhang, H. Pei, L. Li and A. R. Chandrasekaran, *Langmuir*, 2019, **35**, 5050–5053.
3 S. Juul, F. Iacovelli, M. Falconi, S. L. Kragh, B. Christensen, R. Frøhlich, O. Franch, E. L. Kristoffersen, M. Stougaard, K. W. Leong, Y.-P. Ho, E. S. Sørensen, V. Birkedal, A. Desideri and B. R. Knudsen, *ACS Nano*, 2013, **7**, 9724–9734.
4 R. E. Kohman and X. Han, *Chem. Commun.*, 2015, **51**, 5747–5750.
5 F. N. Gür, S. Kempter, F. Schueder, C. Sikeler, M. J. Urban, R. Jungmann, P. C. Nickels and T. Liedl, *Adv. Mater.*, 2021, **33**, 2101986.
6 A. R. Chandrasekaran and K. Halvorsen, *Nanoscale Adv.*, 2019, **1**, 969–972.
7 S. Li, Q. Jiang, S. Liu, Y. Zhang, Y. Tian, C. Song, J. Wang, Y. Zou, G. J. Anderson, J.-Y. Han, Y. Chang, Y. Liu, C. Zhang, L. Chen, G. Zhou, G. Nie, H. Yan, B. Ding and Y. Zhao, *Nat. Biotechnol.*, 2018, **36**, 258–264.
8 R. Peng, X. Zheng, Y. Lyu, L. Xu, X. Zhang, G. Ke, Q. Liu, C. You, S. Huan and W. Tan, *J. Am. Chem. Soc.*, 2018, **140**, 9793–9796.
9 Y. Hu, Y. Jia, Y. Yang and Y. Liu, *RSC Adv.*, 2023, **13**, 9003–9009.
10 H. Yan, X. Zhang, Z. Shen and N. C. Seeman, *Nature*, 2002, **415**, 62.
11 H. Zhong and N. C. Seeman, *Nano Lett.*, 2006, **6**, 2899–2903.
12 S. Liao and N. C. Seeman, *Science*, 2004, **306**, 2072–2074.
13 B. Chakraborty, N. Jonoska and N. C. Seeman, *Chem. Sci.*, 2011, **3**, 168–176.
14 H. Gu, J. Chao, S.-J. Xiao and N. C. Seeman, *Nature*, 2010, **465**, 202–205.
15 Z. Shen, H. Yan, T. Wang and N. C. Seeman, *J. Am. Chem. Soc.*, 2004, **126**, 1666–1674.
16 K. A. Afonin, D. J. Cieply and N. B. Leontis, *J. Am. Chem. Soc.*, 2008, **130**, 93–102.

17 A. R. Chandrasekaran, J. Vilcapoma, P. Dey, S. W. Wong-Deyrup, B. K. Dey and K. Halvorsen, *J. Am. Chem. Soc.*, 2020, **142**, 6814–6821.
18 C. Liu, N. Jonoska and N. C. Seeman, *Nano Lett.*, 2009, **9**, 2641–2647.
19 B. Chakraborty, R. Sha and N. C. Seeman, *PNAS*, 2008, **105**, 17245–17249.
20 A. R. Chandrasekaran, R. Trivedi and K. Halvorsen, *Cell Rep. Phys. Sci.*, 2020, **1**, 100117.
21 J. Bucci, P. Irmisch, E. Del Grosso, R. Seidel and F. Ricci, *J. Am. Chem. Soc.*, 2022, **144**, 19791–19798.
22 J. Bucci, P. Irmisch, E. Del Grosso, R. Seidel and F. Ricci, *J. Am. Chem. Soc.*, 2023, **145**, 20968–20974.
23 S. Agarwal and E. Franco, *J. Am. Chem. Soc.*, 2019, **141**, 7831–7841.
24 H. Faheem, J. Mathivanan, H. Talbot, H. Zeghal, S. Vangaveti, J. Sheng, A. A. Chen and A. R. Chandrasekaran, *Nucleic Acids Res.*, 2023, **51**, 4055–4063.

